ANASLYSIS OF NANOELECTROMECHANICAL SYSTEM BASED MICROMACHINED SENSOR

Abstract

In this paper the investigation of membrane of CMUT device has been analyze systematically. Here the resonance frequency has been detected/evaluated which can be appropriate to make the device. The mechanical impedance of the circular membrane is found nearly equal to acoustic impedance of air which makes the CMUT more preferable in a device. The resonance frequency is found here with and without intrinsic stress which are being used to determine the stress area. Here also for diverse gaseous, liquid and solid substances the acoustic impedance value is different with which we will get different equivalent impedance. It has been found that the equivalent resistance increases from gaseous particles to liquid and to the solid.

Keywords: MEMS/NEMS; Ultrasonic Sensor; CMUT, Micromachined Sensor

Authors

Prof. Niladri Pratap Maity
Professor
National Institute Technical Teachers Training and Research (NITTTR)
Kolkata, West Bengal, India.
maity_niladri@rediffmail.com

Reshmi Maity
Department of Electronics & Communication Engineering
Mizoram University (A Central University)
Aizawl, India.
reshmidas_2009@rediffmail.com

I. INTRODUCTION

The name MEMS originated from United States, it is known as Microsystems Technology (MST) in Europe and micro machines in Asia. Silicon is used in the production of components of MEMS. It is the combination of semiconductor processing and mechanical engineering at a very small scale. A gold resonating MOS gate structure in 1967 was the first MEMS device, it firmly comes in work in the middle of 1980's and now it emerged in real-world applications. The development of IC technologies can now produce chips with features as small is 0.1µm. MEMS consist of four components microstructures, microsensors, microactuators and microelectronics and all are integrated on same silicon chip. Microsensors are used for measuring the physical parameters and are engaged to witness the progressive effects of the atmosphere. Microactuator is based on the micro movement and there are two types of actuations translational and rotational. There the microactuators that are commonly available, they are: Mechanical actuators, Thermal actuators, Electrostatic actuators, Magnetic actuators. MEMS are also referred as Microsystem technology (MST).

Ultrasonic is today applied in medical diagnosis such as Sonography, Lithotripsy, Ultrasonic surgical instruments (USI), high-intensity therapeutic ultrasound (HIFU), ultrasonic scalers and Cavitron ultrasonic surgical aspirator (CUSA). The ultrasonic wave does not involve harmful wave radiation and is also painless. The acoustic streaming is induced in the form of liquid by the ultrasound is affected by the microbial action and the bacteria that can modify the physiochemical parameters of liquid can be distinguished from side to side the use of ultrasonic waves. Ultrasonic waves get reflected, refracted and absorbed just like an ordinary sound waves. The speed of ultrasonic wave is further in compressed media and they work on the property of lights, if the ultrasonic waves enter from rarer to denser medium then it bend away from the normal. Similarly when from denser to rarer then it bends towards the normal. They are high frequency waves and have high energy content and have constant velocity in homogeneous medium. They can produce heating effect when passed through the substances.

II. CAPACITIVE MICRO-MACHINED ULTRASONIC TRANSDUCER (CMUT)

Ultrasonic sensors are very commonly used in today's day to day world like in cars for detecting it's locations, it is also used in ultrasound imaging, UAV (unmanned aerial vehicle) navigations. Some sensors are also used to identify high-pressure gas otherwise liquid leakages and these devices convert the audio from the transducer to human hearing range. Qualcomm manufactured ultrasonic finger sensor which is scalable to any size on the basis of transistor film transistor (TFT). There are some methods that produce ultrasonic waves and they are: Magneto-striction oscillator, Piezoelectric oscillator and Micro-machined ultrasonic transducer (MUT). Out of all the three methods micro-machined ultrasonic transducer is mostly used for good imaging like 2-dimensional and 3-dimentional imaging.

CMUTs are used for receiving and transmitting acoustic signals in ultrasonic range. It was first introduced in 1990. CMUT is mostly used in medical imaging. CMUTs are manufactured in different shapes and sizes. The complications in fabrication procedures have been resolved by many scientist and they are coming with many new approaches. When the CMUT is loaded in liquid medium then more than 100 % frictional bandwidth can be achieved easily. They have poorer mechanical impedance than that of piezoelectric

transducers and it gives healthier coupling with medium and higher bandwidth. It reduces size of the devices and the noise in it. They are of 2-dimensional and 3-dimensional array and can form 2-D and 3-D images for medical imaging. It performs better in terms of bandwidth and sensitivity.

It comprises of silicon or Si_3N_4 membrane or silicon substrate using micromachining skill shown in Fig.1. In transmitting mode, an alternating voltage is applied among the back plate of substrate, membrane and electrostatic forces that is formed cause a vibration on the membrane, sending out the ultrasound at the frequency of modulation. In receiving mode, the ultrasonic wave vibrates the membrane and the change in capacitance is detected.

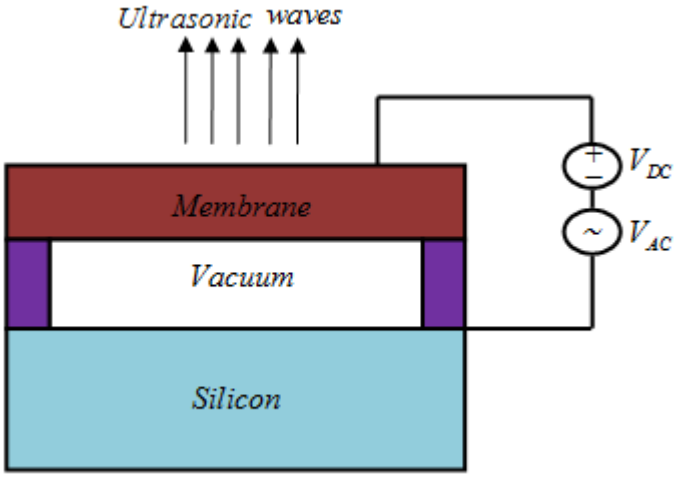

Figure 1: CMUT Device Structure and Principle

In the year 1994, B. T. Khuri-Yakub and Mathew I. Haller from Stanford University worked on the technology Surface Micro-machined Electrostatic Ultrasonic Air Transducer [1]. The paper describes the fabrication of the electrostatic transducer using silicon surface micromachining. After that Khuri-Yakub along with his members analysed the realization of capacitive transducers with the centre frequencies ranging from 1 MHz to 12 MHz. After that the work progressed on Surface Micro-machined Capacitive Ultrasonic Transducers [2]. In the starting year of 21st century researchers worked on characterization of one dimensional (1-D) array in immersion transducer [3-9]. The 1-D CMUT array element of $275\times5600-\mu m$ is experimentally characterized. The receiver transducer has $0.28\,fm/\sqrt{Hz}$ of displacement sensitivity and the transmitter transducer produces $5kPa/V$ of output pressure at the surface of the transducer at 3 MHz with 35 V of DC bias. The bandwidth is more than 100% around 3MHz that is suitable for ultrasound imaging. The acoustical cross coupling between array elements are being modified using several methods like trench isolation and wafer thinning. In the year 2003, B. T. Khuri-Yakub along with his research members proposed the new method to fabricate CMUT with wafer bonding technique [10]. This new technique is very promising to fabricate CMUTs in various dimensions and to operate in air and water at different frequencies.

The CMUT technology is improving day by day along with its imaging system. The photoacoustic imaging provides high contrast with different light absorption characteristics.

The researchers used a vessel like photoacoustic imaging phantom which consist of three 1.3 mm diameter tubes intimate tissue imitating material. Two-dimensional CMUT array enables the volumetric imaging and reduces the drawbacks of mechanically scanned systems. CMUT technology with photoacoustic imaging have number of benifits such as it gives wide bandwidth, ease in integration with electronics, helps in early detection of cancer, etc.

Ultrasonic transducers are now widespread and used in low intensity applications. Therefore, researchers fabricate the silicon carbide based CMUTs [11]. There is a sparse 2-D CMUT ring arrays for getting the high resolution since the volumetric imaging is becoming more popular in medical tools and this CMUT array is integrated in endoscope [12]. In the fabrication on Quad ring capacitive micro-machined ultrasound transducers (CMUTs) there are four self-determining concentric rings in arrays containing 128 elements operating at dissimilar centre frequencies but for endoscope only one concentric ring are used at 4 MHz. Here, the custom charge-amplifier ASICs were used for reducing the noise and this CMUT endoscope has been used for 3-D imaging.

III. MATHEMATICAL ANALYSIS

We have considered the Mason's analysis [13] for circular membrane,

$$\frac{(Y_0+T)l_t^3}{12(1-\sigma^2)}\nabla^4 x(r)-l_tT\nabla^2 x(r)-P-l_t\rho\frac{d^2x(r)}{dt^2}=0 \quad (1)$$

$Y_0 =$ Young's Modulus and $\sigma =$ Poisson's ratio. After calculation,

$$\frac{D}{l_tT}\nabla^4 u-\nabla^2 u-\frac{P}{l_tT}-\frac{\rho}{T}\frac{d^2u}{dt^2}=0 \quad (2)$$

We know $\nabla^2 u =$ Laplacian operator, $T =$ Tension. Therefore, $\nabla^4 u=\nabla^2\{\nabla^2 u\}=(\nabla^2 u)^2$ so,

$$\frac{D}{l_tT}\left(\frac{d^2u}{dr^2}+\frac{1}{r}\frac{du}{dr}\right)^2-\left(\frac{d^2u}{dr^2}+\frac{1}{r}\frac{du}{dr}\right)-\frac{P}{l_tT}-\frac{\rho}{T}\frac{d^2u}{dt^2}=0 \quad (3)$$

where r = radical position measured from the centre. Equating the equation we can get ($x(r) =$ displacement of the membrane, $\rho =$ density of the material, $P =$ pressure on the membrane)

$$\frac{D}{l_tT}\left(\frac{d^2u}{dr^2}+\frac{1}{r}\frac{du}{dr}\right)^2 e^{j\omega t}-\left(\frac{d^2u}{dr^2}+\frac{1}{r}\frac{du}{dr}\right)e^{j\omega t}+\frac{\rho}{T}\omega^2 u e^{j\omega t}-\frac{P}{l_tT}e^{j\omega t}=0 \quad (4)$$

Let us take $\lambda=-k_1^2$, then it will become.

$$r^2R''(r)+rR'(r)+r^2k_1^2R(r)=0 \quad (5)$$

Or $$r^2\frac{d^2u}{dr^2}+r\frac{du}{dr}+r^2k_1^2u=0 \quad (6)$$

Again let $k_2'^2=\frac{\omega^2\rho}{T}$

$$\left(\frac{d^2u}{dr^2}+\frac{1}{r}\frac{du}{dr}\right)-k_2'^2u=-\frac{P}{l_tT} \quad (7)$$

Therefore solution will become,

$$x(r)=AJ_0(k_1r)+BI_0(k_2r)-\frac{P}{\omega^2\rho l_t} \quad (8)$$

At the moment to decide the constant A and B there are two boundary conditions that are essential.

Condition 1:

When $r=a,\ x=0$ then equation will be,

$$x(a)=AJ_0(k_1a)+BI_0(k_2a)-\frac{P}{\omega^2\rho l_t} \quad (9)$$

$$0=AJ_0(k_1a)+BI_0(k_2a)-\frac{P}{\omega^2\rho l_t} \quad (10)$$

$$AJ_0(k_1a)+BI_0(k_2a)=\frac{P}{\omega^2\rho l_t} \quad (11)$$

Condition 2:

$$\frac{dx}{dr}=0$$

Since, $r=a$

$$\frac{dx}{da}=0$$

$$\frac{d}{da}\left[AJ_0(k_1a)+BI_0(k_2a)-\frac{P}{\omega^2\rho l_t}\right]=0$$

$$-Ak_1J_1(k_1a)+Bk_2I_1(k_2a)=0 \quad (12)$$

$$-Ak_1J_1(k_1a) = -Bk_2I_1(k_2a)$$

$$A = \frac{k_2I_1(k_2a)}{k_1J_1(k_1a)}B \tag{13}$$

So, A and B will be,

$$A = \frac{P}{\omega^2 \rho l_t}\left[\frac{k_2I_1(k_2a)}{k_2I_1(k_2a)J_0(k_1a)B + k_1BI_0(k_2a)J_1(k_1a)}\right] \tag{14}$$

$$B = \frac{P}{\omega^2 \rho l_t}\left[\frac{k_1J_1(k_1a)}{k_2I_1(k_2a)J_0(k_1a) + k_1I_0(k_2a)J_1(k_1a)}\right] \tag{15}$$

The average velocity at the surface is given as:

$$v_a = \frac{v_t}{\pi a^2} \tag{16}$$

That is equal to

$$v_a = \frac{j\omega 2\pi \int_0^a \frac{P}{\omega^2 \rho l_t}\left[\frac{k_2J_0(k_1r)I_1(k_2a) + k_1I_0(k_2r)J_1(k_1a)}{k_2J_0(k_1a)I_1(k_2a) + k_1I_0(k_2a)J_1(k_1a)} - 1\right]rdr}{\pi a^2} \tag{17}$$

Employing the integral

(18)

$$\int rJ_0(kr)dr = \frac{J_1(kr)}{k}$$

$$v_a = \frac{j\omega 2\pi\left\{\frac{P}{\omega^2 \rho l_t}\left[\frac{k_2a\frac{J_1(k_1a)}{k_1}I_1(k_2a) + k_1a\frac{I_1(k_2a)}{k_2}J_1(k_1a)}{k_2J_0(k_1a)I_1(k_2a) + k_1I_0(k_2a)J_1(k_1a)} - \frac{a^2}{2}\right]\right\}}{\pi a^2}$$

To calculate the mechanical impedance, v_a is now equal to,

$$v_a = \frac{\frac{jP\pi a^2}{\omega\rho l_t}\left[\frac{\frac{2}{a}\left(\frac{k_2}{k_1}+\frac{k_1}{k_2}\right)J_1(k_1a)I_1(k_2a)}{k_2J_0(k_1a)I_1(k_2a)+k_1I_0(k_2a)J_1(k_1a)}-1\right]}{\pi a^2}$$

Therefore, the average velocity will become:

$$v_a = \frac{jP}{\omega\rho l_t}\left[\frac{\frac{2}{a}\left(\frac{k_2}{k_1}+\frac{k_1}{k_2}\right)J_1(k_1a)I_1(k_2a)}{k_2J_0(k_1a)I_1(k_2a)+k_1I_0(k_2a)J_1(k_1a)}-1\right] \tag{19}$$

The proportion of pressure to the velocity is demarcated as mechanical impedance and is represented as Z_m

$$Z_m = \frac{P}{v_a} = \frac{P}{\frac{jP}{\omega\rho l_t}\left[\frac{\frac{2}{a}\left(\frac{k_2}{k_1}+\frac{k_1}{k_2}\right)J_1(k_1a)I_1(k_2a)}{k_2J_0(k_1a)I_1(k_2a)+k_1I_0(k_2a)J_1(k_1a)}-1\right]} \tag{20}$$

Since, $\frac{1}{j} = -j$

The mechanical impedance of circular membrane is given as:

$$Z_m = -j\omega\rho l_t\left[\frac{ak_1k_2\left(k_2J_0(k_1a)I_1(k_2a)+k_1I_0(k_2a)J_1(k_1a)\right)}{2\left(k_1^2+k_2^2\right)J_1(k_1a)I_1(k_2a)-ak_1k_2\left(k_2J_0(k_1a)I_1(k_2a)+k_1I_0(k_2a)J_1(k_1a)\right)}\right] \tag{21}$$

The mechanical impedance of the membrane is insignificant compared to acoustic impedance of medium that is necessary for efficient power transfer. Now the resonance frequency for this mode is,

$$f_{r2} = 2.4048\frac{1}{2\pi a}\sqrt{\frac{T}{\rho}} \tag{22}$$

IV. RESULTS AND DISCUSSION

The different values for different parameters are substituted in the above solved equations and the graphs are plotted for different profiles [14]. Different parameters values are being taken for the paper defines the characterization of the device and the device performance in Table 1.

Table 1: Values and units of Parameters

Parameters	Values
a	$25\times10^{-6}m$
P	$1N/m^2$
Y_0	$3.2\times10^{11}N/m^2$
l_t	$0.6\times10^{-6}m$
T	$280\times10^{6}N/m^2$
ε_0	$8.85\times10^{-12}F/m$
σ	0.263
l_a	$0.2\times10^{-6}m$
ρ	$3270kg/m^3$

The Fig. 2 shows that the variation is taken between displacement and frequency where it is found that there is a peak resonance frequency at 6.7 MHz.

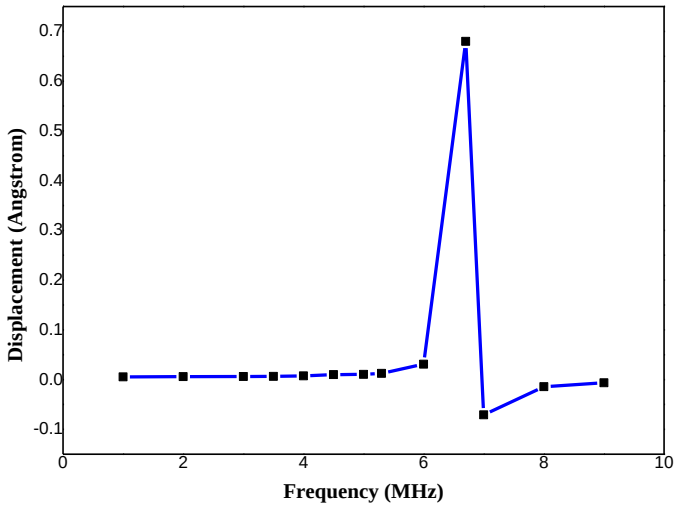

Figure 2: Variations of Displacement with Frequency

The Fig. 3 is showing that displacement fluctuates with the radius and it demonstrations that the displacement of membrane is lessening with the upsurge in the radius.

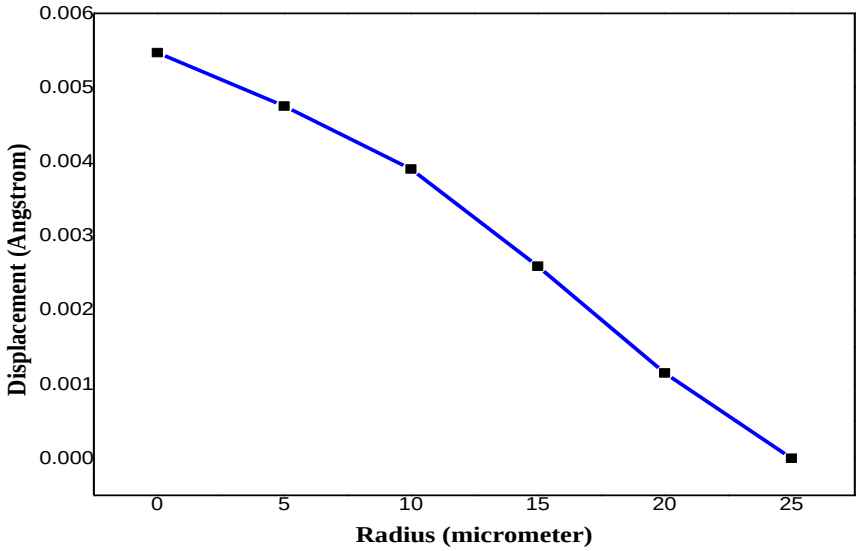

Figure 3: Variations of Displacement with Radius

In Fig.4, it is showing that the mechanical impedance of the membrane reductions with the upsurge in the frequency to the point of resonance frequency at 6.7 MHz wherever the mechanical impedance is approximately near to the acoustic impedance of the air and later increases gradually.

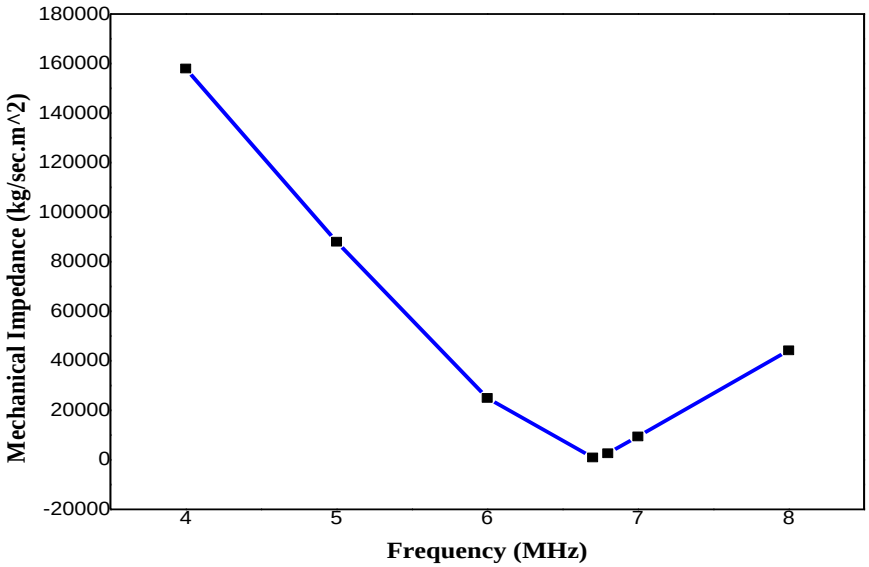

Figure 4: Variations of Mechanical Impedance with Frequency

The coupling factor is intensifications with the increase in DC voltage as shown in Table 2. As soon as the radius of the membrane upsurges the area also surges and the coupling factor rises with the escalation in the value of radius/area with respect to the increase in DC voltage.

Table 2: Coupling Factor with DC Voltage While Changing the Radius/Area

SL.NO	DC Voltage	Coupling factor at	Coupling factor at	Coupling factor at
	(volts)	η	η_1	η_2
1.	10	1.40E-07	3.40E-08	5.95E-07
2.	20	2.90E-07	6.85E-08	1.19E-06
3.	30	4.30E-07	1.03E-07	1.79E-06
4.	40	5.80E-07	1.37E-07	2.38E-06
5.	50	7.20E-07	1.71E-07	2.98E-06
6.	60	8.70E-07	2.05E-07	3.57E-06
7.	70	1.01E-06	2.74E-07	4.17E-06

The Table 3 depicts that despite the fact exchanging the thickness of the membrane, coupling factor also changes. Again the thicknesses of the membrane upsurges from the coupling factor will shrinkage with respect to intensification in DC Voltage.

Table 3: Coupling factor with DC voltage while changing membrane thickness

SL.NO	DC Voltage	Coupling factor at	Coupling factor at	Coupling factor at
	(volts)	η	η_1	η_2
1.	10	1.40E-07	1.52E-07	1.37E-07
2.	20	2.90E-07	3.03E-07	2.75E-07
3.	30	4.30E-07	4.55E-07	4.12E-07
4.	40	5.80E-07	6.06E-07	5.49E-07
5.	50	7.20E-07	7.58E-07	6.87E-07
6.	60	8.70E-07	9.10E-07	8.24E-07
7.	70	1.01E-06	1.06E-06	9.61E-07

In Table. 4 it shows that when the gap thickness increases the coupling factor with DC voltage will decrease whereas the increase in DC voltage increases the coupling factor.

Table 4: Coupling Factor with Respect to DC Voltage While Changing Gap Thickness

SL.NO	DC Voltage	Coupling factor at	Coupling factor at	Coupling factor at
	(volts)	η	η_1	η_2
1.	10	1.40E-07	4.90E-07	6.73E-08
2.	20	2.90E-07	9.80E-07	1.35E-07
3.	30	4.30E-07	1.47E-06	2.02E-07
4.	40	5.77E-07	1.96E-06	2.69E-07
5.	50	7.20E-07	2.45E-06	3.36E-07
6.	60	8.70E-07	2.94E-06	4.04E-07
7.	70	1.01E-06	3.43E-06	4.71E-07

The resonance frequency decreases with the intensification in radius in together the two different formulas with intrinsic stress and without intrinsic stress (Fig. 5).

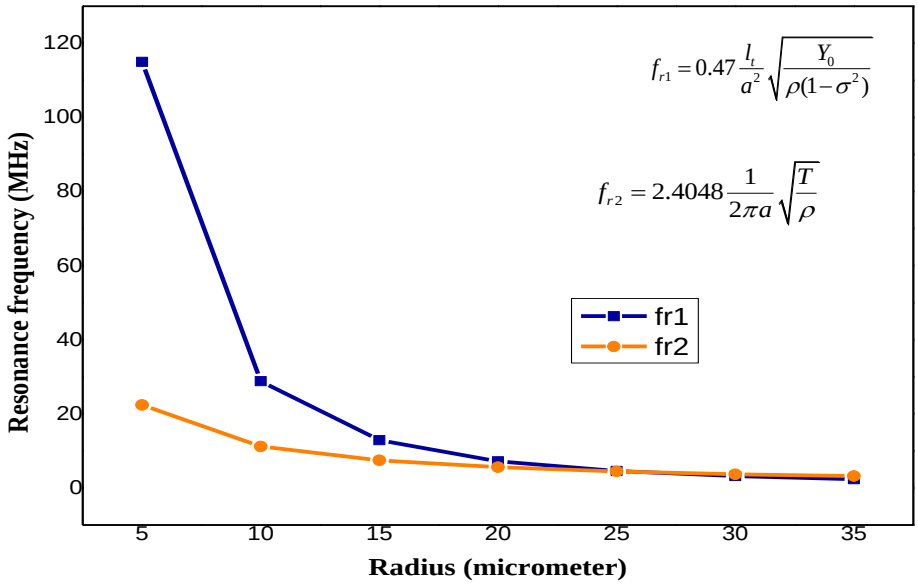

Figure 5: Variations in Resonance Frequency With Radius

The Table 5 depicts that for diverse gaseous, liquid and solid substances the acoustic impedance value is different with which we will get different equivalent impedance. The equivalent resistance increases from gaseous particles to liquid and to the solid.

Table 5: Equivalent Resistance with Respect to Acoustic Impedance

SL.NO.	Names	Acoustic impedance Z_a	Equivalent resistance
1.	Air	400	1359.2
2.	Oxygen	449	1525.7
3.	Castor oil	1.43E+06	4.86E+06
4.	Water	1.48E+06	5.03E+06
5.	Sea water	1.54E+06	5.23E+06
6.	Glycerine	2.42E+06	8.22E+06
7.	Aluminium	1.70E+07	5.78E+07
8.	Steel	4.70E+07	1.60E+08

V. CONCLUSION

In this chapter the membrane of CMUT when subjected to AC bias then displacement of membrane decreases with the intensification in the radius of membrane. Here the resonance frequency is found at 6.7 MHz which can be suitable to make a device. The mechanical impedance of the circular membrane is found nearly equal to acoustic impedance of air which makes the CMUT more preferable in a device. The resonance frequency is found here with and without intrinsic stress which are being used to determine the stress area. In the electrical equivalent circuit of CMUT the acoustic and mechanical impedance must kept in

series instead of parallel, so that the total load didn't get zero. It is also clear that for larger bandwidth the thickness of membrane and gap thickness must be small as possible and the DC bias voltage should be kept high.

REFERENCES

[1] M. I. Haller and B. T. Khuri-Ykub, "A surface micromachined electrostatic ultrasonic air transducer," in Ultrasonic Symposium, Cannes, France, pp. 1241-1244, 1994.
[2] Avik Ghosh Dastidar, Reshmi Maity, R. C. Tiwari, D. Vidojevic, T. Kevkic, V. Nikolic, S. Das, and N. P. Maity, "Squeeze Film Effect in Surface Micromachined Nano Ultrasonic Sensor for Different Diaphragm Displacement Profiles', Sensors, vol. 23, no. 10, p. 113712, https://doi.org/10.3390/s23104665.
[3] Avik Ghosh Dastidar, M. Pal, R. C. Tiwari, R. Maity, N. P. Maity, "An efficient electrostatic actuation model for MEMS-based ultrasonic transducers with fringing effect," Microsystem Technologies, https://doi.org/10.1007/s00542-023-05412-1, 2023.
[4] R. Maity, N. P. Maity, K. S. Rao, G. Sravani, K. Guha, "Design of Single Cell Membrane Shape and Array Configuration for MEMS Based Micromachined Ultrasonic Sensor to Improve the Performance: A Three Dimensional Model Characterization," Transactions on Electrical and Electronic Materials, vol. 22, pp. 809-820, 2021, https://doi.org/10.1007/s42341-021-00303-6.
[5] Igal Ladabaum, Xuecheng Jin, Hyongsok T. Soh, Abdullah Atalar and Butrus T. Khuri-Yakub, "Surface micromachined capacitive ultrasonic transducers" IEEE Trans on Ultras. Ferroelect and Frequency control, vol. 45, no. 3, pp 678-690, May 1998.
[6] M. Pal, C. Lalengkima, R. Maity, S. Baishya, N. P. Maity, "Effects of fringing capacitances and electrode's finiteness in improved SiC membrane based micromachined ultrasonic transducers," Microsystem Technologies, vol. 27, pp. 3679-3691, 2021, https://doi.org/10.1007/s00542-020-05135-7.
[7] Reshmi Maity, N. P. Maity, and S. Baishya, "An Efficient Model of Nanoelectromechanical Systems Based Ultrasonic Sensor with Fringing Field Effects," IEEE Sensor Journals, Vol. 20, No. 4, pp. 1746-1753, 2020, **DOI:** 10.1109/JSEN.2019.2948795.
[8] M. Pal, N. P. Maity, S. Baishya, R. Maity, "Performance Analysis of Nano-Electro-Mechanical-System Ultrasonic Sensor with Fringing Field Effects," Transactions on Electrical and Electronic Materials, vol. 22, pp. 757-763, 2021, https://doi.org/10.1007/s42341-021-00297-1.
[9] Reshmi Maity, Shonkho Suvra, Santanu Maity and N. P. Maity, "Collapse Voltage Analysis of Central annular Ring Metallized Membrane Based MEMS Micromachined Ultrasonic Transducer", Microsystem Technologies , vol. 26, pp. 1001-1009, 2020, https://doi.org/10.1007/s00542-019-04613-x.
[10] Y. Huang, A. S. Ergun, E. Haeggstrom and B. T. Khuri-Yakub, " New fabrication process for Capacitive Micromachined Ultrasonic Transducers," in IEEE Ultrasonic Symposium, pp. 522-525, 2003.
[11] Qing Zhang, Paul-Vahe Cicek, Karim Allidina, Frederic Nabki and Mourad N. El-Gamel, "Surface-Micromachined CMUT using low-temperature deposited Silicon Carbide membranes for above-IC integration," Journel of Microelectromechanical systems, vol. 23, No. 2, April 2014.
[12] Azadeh Moini, Amin Nikoozadeh, Jung Woo Choe, Chienlier Chang, Douglas N. Stephens, David J. Sahn and Pierre T. Khuri-Yakub, "Fully integrated 2D CMUT ring arrays for Endoscopic Ultrasound," in IEEE International Ultrasonic Symposium Proceedings, 2016.
[13] W. P. Mason, Electromechanical Transducers and Wave Filters. New York: Van Nostrand, 1942
[14] R. Maity, K. Gogoi, N. P. Maity, "Micro-electro-mechanical-system based capacitive ultrasonic transducer as an efficient immersion sensor," Microsystem Technologies, Vol. 25, pp. 4663–4670, 2019, https://doi.org/10.1007/s00542-019-04384-5.

